Journal of Achievements in Materials and Manufacturing Engineering
VOLUME 59
ISSUE 1
July
2013

About heat treatment and properties of Duplex Stainless Steels

M. Rosso*, I. Peter, D. Suani
Department of Applied Science and Technology,
Institute of Science and Engineering of Materials for the Innovative Technologies,
ALTO - Metallurgy Group, Alessandria Campus & Torino,
Politecnico di Torino, Corso Duca degli Abruzzi, 24, 10129 Torino, Italy
* Corresponding e-mail address: mario.rosso@polito.it

Received 03.05.2013; published in revised form 01.07.2013

Properties

ABSTRACT

Purpose: of this paper is to review the effect of heat treatments and of strain hardening on microstructure and properties of superduplex stainless steels.
Design/methodology/approach: Annealing and strain hardening treatments influences microstructures and properties.
Findings: The characteristics and the properties of the industrially employed superduplex grade has been discussed, moreover the presence and the precipitation of sigma phase has been highlighted through ageing treatments.
Research limitations/implications: : Based on the up to date achieved outcomes, it appears that a quite homogeneous and good mechanical properties can be obtained controlling the composition and the heat treatment and strain hardening parameters.
Practical implications: The major implication is related to the transfer toward the proper choice of correct parameters for working the duplex grades.
Originality/value: to supply deeper information with respect to those available in literature, which does not clearly indicate what amount of secondary phases existing in duplex stainless steel microstructure can be acceptable.
Keywords: Heat treatments; Strain hardening; Superduplex stainless steels; Mechanical properties; Microstructures

Reference to this paper should be given in the following way:
M. Rosso, I. Peter, D. Suani, About heat treatment and properties of Duplex Stainless Steels, Journal of Achievements in Materials and Manufacturing Engineering 59/1 (2013) 26-36.

1. Introduction

Stainless steel is the name given to a family of corrosion and heat resistant steels containing a minimum of 10.5% chromium. Just as there is a range of structural and engineering carbon steels meeting different requirements of strength, weldability and toughness, so there is a wide range of stainless steels with progressively higher levels of corrosion resistance and strength.

The available grades of stainless steel can be classified into five basic families: ferritic, martensitic, austenitic, duplex and precipitation hardenable. The division based on microstructure is useful because the members within one family tend to have similar physical and mechanical properties. However, the properties for one family can be very different from the properties of another family. For example, austenitic stainless steels are non-magnetic, while ferritic and duplex stainless steels are magnetic.

Duplex stainless steels typically are dual phase structured alloy, that is their microstructure consists of a mixture of austenitic and delta ferritic grains. This results is achieved from the controlled addition of alloying elements, each offering specific attributes in respect of strength and ability to resist different environments.

Duplex stainless steels contain increased amount of chromium (18-28%) and decreased (as compared to austenitic steels) amount of nickel (4.5-8%) as major alloying elements. As additional alloying element molybdenum is used in some of Duplex steels. Since the quantity of nickel is insufficient for formation of fully austenitic structure, the structure of Duplex steels is mixed: austenitic-ferritic and important improvements have been realized over the last decade. In particular, further additions of Nitrogen have been made improving weldability.

The high level of alloying elements of these stainless alloys, such as chromium, nickel, molybdenum, and nitrogen, should be properly balanced in order to achieve similar volumetric fractions of both phases and to give, both ferrite and austenite, a proper corrosion and mechanical resistance. Yield strength of these steels is more than twice that of the single-phase stainless steels either ferritic or austenitic. They also have superior toughness and ductility when compared to the ferritic and martensitic types, in addition to superior intergranular and stress corrosion resistance in comparison to the austenitic type. This favorable combination of properties makes this class of stainless steels widely employed in oil and gas, petrochemical, pulp and paper, and pollution control industries. They are frequently used in aqueous solutions containing chlorides, where they have substituted with advantage (major reductions in weight and welding time) the austenitic stainless steels that are more susceptible to stress and pitting corrosion.

As well known the alloys work harden if cold formed; however for these compositions even the strain produced from welding can work harden the material particularly in multi pass welding. Therefore a full solution anneal is advantageous, particularly if low service temperatures are foreseen.

Duplex stainless steels solidify initially as "δ" ferrite, then the austenite forms on further cooling in the solid state at the grain boundaries between 1400 and 1200°C, as indicated by the phase diagram illustrated in Fig. 1 [1]. Depending upon the composition, a varying amount of austenite is expected to form as the last material solidifies.

Additional austenite forms by a solid-phase transformation during subsequent annealing. Consequently, an annealed product contains more austenite than the as-cast or the as-welded material. A sufficient amount of austenite must be maintained to provide satisfactory corrosion resistance and mechanical properties. This amount of austenite may vary with the service application and with the alloy composition and its thermal history.

In modern raw material the balance should be 50/50 for optimum corrosion resistance, particularly resistance to stress corrosion cracking. However the materials strength is not significantly affected by the ferrite/austenite phase balance.

The importance of dual phase stainless steel have stimulated also the development of studies related to the powder metallurgy technology for the production of near net shape components by sintering. In particular, it was demonstrated [2-7] a very favourable and promising PM way starting from austenitic X2CrNiMo17-2-2, martensitic X6Cr13 powders by controlled addition of alloying elements, such as Cr, Ni, Mo, Cu in the right quantity to obtain the chemical composition of the structure similar to biphasic ones produced by traditional melting routes.

The main problem with Duplex alloys is that they very easily form brittle intermetallic phases, such as Sigma, Chi and Alpha Prime. These phases can be formed rapidly, typically in 100 seconds at 900°C. However, it was verified that shorter exposures cause also a drop in toughness. This fact has been attributed to the formation of sigma on a microscopic scale. Moreover, prolonged heating in the range 350 to 550°C can cause at 475°C temper embrittlement due to α' precipitation. For this reason the maximum recommended service temperature for duplex is about 280°C.

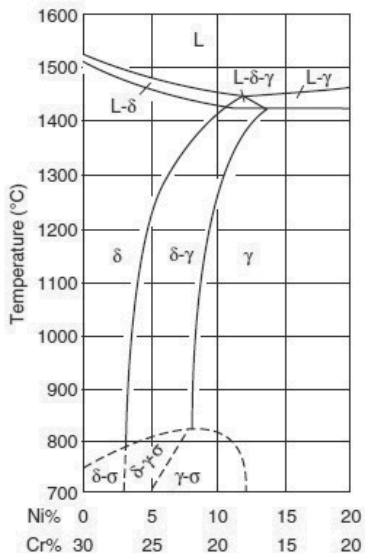

Fig. 1. Section of the ternary Fe-Cr-Ni (wt. %) diagram at 65 w.t.% Fe [1]

Sigma (55Fe - 45Cr) can be a major problem when welding thin walled small bore pipe made of super duplex, although it can occur in thicker sections. It tends to be found in the bulk of the material rather than at the surface, therefore it probably has more effect on toughness than corrosion resistance. Sigma can also occur in thick sections, such as castings that have not been properly solution annealed [8]. However most standards accept that deleterious phases, such as sigma, chi and laves, may be tolerated if the strength and corrosion resistance are satisfactory.

Nitrogen is a strong austenite former and largely responsible for the balance between ferrite and austenite phases and the materials superior corrosion resistance.

Duplex and Super Duplex grades are alloys containing 20-30% Cr, 3-10% Ni, 0.5-7.5% Mo and 0-3% Cu and consisting of 30 to 70% ferrite with the remainder austenite. The carbon content is generally kept below 0.04% and the alloys are quenched from above 1050°C to avoid carbide precipitation; this also avoids the formation of other undesirable intermetallic phases such as a sigma phase. The addition of nitrogen, in association with argon/oxygen decarburization, causes the stable amount of austenite to form more rapidly at higher temperatures; it also stabilizes and strengthens the austenite phase [9-11].

Moreover, nitrogen slows down the formation of intermetallic phases [12-14]. The presence of the two phases (austenite and ferrite) in the structure of duplex steels provides high strength and good formability at room temperature, good weldability and exceptional corrosion resistance under severe conditions [9,10,15,16]. In particular, duplex steels have very high resistance to chloride pitting and stress corrosion/cracking which increases with Cr-Mo content, allowing them to be used for severe applications in the oil, gas and petrochemical industries [9,10,15].

Thanks to their advanced complex microstructure, containing ferrite and austenite, and their unique chemical composition based on high volumes of Cr and Mo Duplex stainless steels are now at the forefront of alloy technology and, with additions of nitrogen, the net effect is enhanced intergranular and pitting corrosion resistance. In terms of yield strength and ultimate yield values, the overall results is an organically stronger steel with higher resistance to pitting and cracking from stress corrosion. The properties of Duplex steels are somewhere between the properties of austenitic and ferritic steels and have high resistance to the stress corrosion cracking and to chloride ions attack.

Pitting corrosion resistance in stainless steels is mainly linked to the chromium, molybdenum, and nitrogen contents. At the end of the 1960s, some relationships [16-19] were suggested relating pitting corrosion resistance (PRE) to the content of Cr, Mo and N as indicated by the following equation:

$$PRE = \% Cr + 3.3\% Mo + 16\ \% N \quad (1)$$

where compositions are in wt.%.

Chromium and molybdenum are ferrite formers and they concentrate mainly in ferrite, and nitrogen goes mainly to austenite. In the initial development steps, duplex steels had low nitrogen levels and were quite susceptible to pitting corrosion. Some modern duplex steels have higher nitrogen levels (0.2 to 0.32wt%), which give a higher pitting corrosion resistance to austenite, comparable to ferrite. Here it should be mentioned that an exaggerated increase in the nitrogen level leads to an increase in the austenite level beyond the level adequate for mechanical resistance. For long exposure times in chloride-rich environments, such as seawater, a level of PRE >40 is nowadays considered satisfactory. Alloys containing PRE >40 are known as superduplex. Duplex stainless steels are practically immune to stress corrosion, when compared to austenitic stainless steels. They are also, in general, more resistant to intergranular corrosion.

Numerous duplex compositions having different combinations of mechanical properties, corrosion, and wear resistance are produced with continuous improvements in composition and secondary metallurgy.

2. Embrittlement, sigma phase and microstructural constituents

The additional phases, which can be found in duplex stainless steels, namely σ, χ, α', carbides and nitrides, have generally been studied using isothermal heat treatments in the laboratory, nevertheless and despite numerous studies and related researches [20-24], the effect of specific amount and proper limits of their presence are not yet very clear.

Apart special cases in which duplex stainless steels contain some higher C content, which can generate the presence of carbides networks, the causes of embrittlement phenomena in low C containing duplex stainless steels [25,26] are mainly related to:

- Embrittlement caused by precipitation of the α'-phase, 475°C embrittlement of ferrite
- Embrittlement caused by precipitation of the σ-phase, particularly in the ferrite

During hot working, between 900 and 1200°C, a microstructure forms with alternating ferrite and austenite lamellae. The lamellar microstructure forms because the interface energy of the δ-γ interface is lower than the energies of the δ-δ and the γ-γ grain boundaries.

After solidification, the volume fraction of austenite and ferrite is almost the same. Below 1000°C the proportion of ferrite to austenite can be only slightly modified. Ferrite strengthening occurs by solid solution hardening with preferential participation of chromium, molybdenum, and silicon, whereas austenite is stabilized and strengthened by nitrogen.

The schematic TTT diagram (Fig. 2), as studied by Reick et al. [1], illustrates the high temperatures regions delimitated by C-shaped curves in which sigma (σ) and chi (χ) phases, as well as carbides ($M_{23}C_6$ type) and chromium nitride (Cr_2N) can precipitate, while at lower temperature the precipitation alpha prime (α') can occur. These precipitates increase the hardness and decrease ductility and the toughness. It must be pointed out that σ phase precipitates within the ferrite [1, 25-28].

The precipitation of α' in ferritic and duplex stainless steels has been frequently discussed in the literature [1,25,26,29,30]. These chromium rich precipitates, having a cubic structure, are coherent with ferrite and have an enormous coalescence resistance, even for very long exposure times at the 350 to 550°C temperature range. This renders their detection more difficult, even by transmission electron microscopy [8]. This type of embrittlement leads to a cleavage fracture in the ferritic regions.

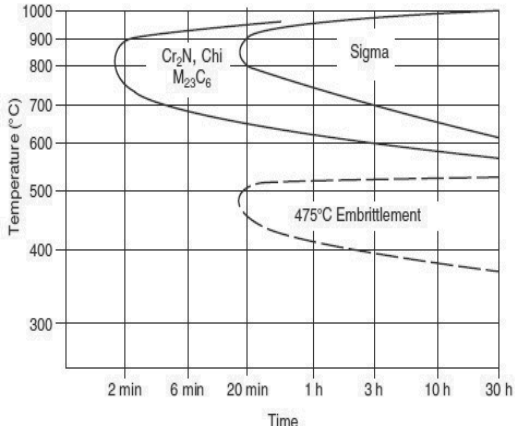

Fig. 2. Schematic TTT diagram showing precipitation of sigma, alpha prime and other phases in duplex stainless steels [1]

Ductility is determined by the austenitic regions and is portrayed by the dimple-like fracture. Austenite volume fraction also plays an important role. Increasing chromium content in the alloy (and thereby the ferrite volume fraction) raises the

sensitivity of the material to this type of embrittlement. The extent of embrittlement increases with aging time in the 350 to 550°C temperature range, while a maximum occurs at about 475°C in correspondence to the possible α' precipitation.

Duplex alloys, owing to the σ phase and α' phase embrittlement, maintain excellent toughness at low temperatures and the upper application temperature is about 280°C for nonwelded alloys, while welded structures must be used down to 250°C or even lower temperatures; in any case the weld-metal behaviour is not as good as the base metal.

As already stated, sigma is a hard, brittle intermetallic phase which is expected to contain iron, chromium and molybdenum in most duplex stainless steels. In these alloys, σ generally can be formed between about 950 and 600°C, with the most rapid formation occurring between 900 and 700°C.

Sigma typically nucleates in the austenite-ferrite grain boundaries and grows into the adjacent ferrite. Often, additional austenite forms in the areas of chromium depletion adjacent to the σ phase. Elements which stabilize ferrite such as chromium, molybdenum and silicon increase the tendency to form the σ phase. On a weight percent basis, molybdenum can promote σ phase formation much more effectively than chromium, particularly at higher temperatures (e.g. about 900°C). Austenite forming elements such as nickel or nitrogen can also accelerate the nucleation and growth of the σ phase, although these elements may reduce the total amount formed.

The alloy elements are portioned, and increased levels of each element tend to be present in the phases they stabilize. As nickel or nitrogen stabilize additional austenite, the reduced amount of ferrite becomes enriched in chromium and molybdenum. As a result, σ phase formation may be reduced by nickel or nitrogen, because of the smaller volume fraction of ferrite.

The σ phase can deplete chromium and molybdenum in surrounding areas and reduce resistance to corrosion. As little as about 1% σ phase may reduce impact toughness, while about 10% can cause complete embrittlement of duplex stainless steels.

The precipitation of sigma phase in stainless steels can occur in the austenitic, ferritic, and ferritic-austenitic phases with duplex structure types. The precipitation of this Fe-Cr-Mo intermetallic, of tetragonal structure with 30 atoms per unit cell, causes loss in toughness and results in the matrix becoming depleted of chromium and molybdenum. While in the austenitic steels, precipitation generally requires hundreds or even thousands of hours and the precipitated volumetric fraction is generally smaller than 5 vol% [31]. Precipitation can be represented by a common precipitation reaction:

$$\gamma \longrightarrow \gamma^* + \sigma \qquad (2)$$

where γ* is a chromium - and molybdenum-depleted austenite, if compared to the original austenite. Precipitation occurs predominantly at grain boundaries, especially at triple points.

In the case of duplex stainless steels, precipitation can be complete in a few hours and consumes all ferrite of the microstructure [32]. Precipitation in this case can be represented by an eutectoid-type reaction:

$$\delta \longrightarrow \gamma^* + \sigma \qquad (3)$$

where γ* is a chromium - and molybdenum-depleted austenite if compared to a nontransformed austenite. Precipitation starts at the δ-γ interface and moves into the ferrite grain.

The quantity, speed, and probably the mode of the sigma-phase precipitation in ferritic stainless steels strongly depend on the steel composition, especially on the chromium and molybdenum contents. Increasing chromium and molybdenum levels displace precipitation start to shorter times and to higher temperatures. Moreover, molybdenum additions can also cause chi (χ)-phase precipitation. It was also observed [33] that sigma and chi-phase precipitations are delayed by aluminum additions and could be eliminated if additions are sufficiently high. Copper has a similar effect on the formation of these two phases [33]. Recent studies [34, 35] on stainless steels showed that the kinetics of sigma phase precipitation is faster than for the austenitic stainless steels, however slower than for the duplex stainless steels. That is, in comparison to austenitic and ferritic stainless steels, precipitation of σ phase in duplex alloys occurs at shorter times, at higher temperatures and larger volume fractions may be formed.

In conclusion, duplex stainless steels are susceptible of embrittlement when σ phase particles are dispersed in the ferritic regions that suffer brittle fracture, and when the α' phase forms also causing embrittlement in the ferrite, leading to cleavage fracture. Moreover, for grades with higher C level, carbide precipitations can form an almost continuous network in the austenitic regions, thereby offering a path for crack propagation. In any case, when embrittlement occurs, material residual ductility is given by the austenitic areas that undergo ductile dimple-like fracture.

Guidelines to provide Duplex Stainless Steels for appropriate applications in critical environments must account for the contribution of alloying, as well as for their side effects. In particular, Cr, Mo and N improve corrosion resistance but increase also the risk of precipitates; then a strict control of the composition and of the treatment parameters is fundamental.

Phase diagrams are important not only to predict the phases that are present in the alloys, but they are also very important as a guide to their heat treatments. However, in complex alloys they do have limitations due to the complexity of the multicomponent thermodynamic calculations and also due to the transformation kinetics that may prevent the attainment of the equilibrium phases. Regarding the first limitation, the number of relevant components is often more than five and published diagrams are rarely found to contain more than four components. As to the second limitation, the diffusion of alloying elements in the solid state can be very slow, especially in the case of austenitic stainless steels, where the precipitation of certain intermetallic compounds can take thousands of hours.

The presence and the equilibrium of austenite, ferrite and sigma phases are shown in the ternary Fe-Cr-Ni diagram in Fig. 3 [36]. It is a basic diagram for stainless steels and shows that a high Cr/Ni ratio sigma phase precipitation may occur during aging at temperatures between 550°C and 900°C. The compositional range of the sigma-phase field increases as the temperature is below 900°C.

Recrystallization kinetics are faster in ferrite than in austenite, despite the higher driving force for the recrystallization in austenite [27]. During hot deformation, at temperatures between 1000 and 1200°C, alternate layers of ferrite and austenite are developed in the microstructure. Phase volumetric fractions must be nearly equal and the volumetric fraction of the minor phase should not be lower than 30% [37].

Because the favourable combination of properties of duplex steels is intrinsically related to its microstructure, it must be

remembered that the volume fraction of each phase is a function of composition and heat treatment. Furthermore, the alloy compositions are adjusted to obtain equal amounts of ferrite and austenite after solution annealing at about 1050°C. Cooling from the solution annealing temperature should be sufficiently fast, generally into water, in order to avoid precipitation of the undesired phases as indicated by TTT diagrams (Figs. 2 and 4). In particular, the TTT diagram of Fig. 4 [38,39] shows the influence of Mo contents on the precipitation of σ and χ phases. The C-shaped curves move from the left to the right as the Mo content decreases. It is evident that the risk of σ and χ phases precipitation became very high when Mo approaches 3.5 wt.%. Moreover, further risk of embrittlement is in the region of 475 °C due to the possible precipitation of alpha prime (α').

It is noteworthy that the risks of precipitations of the mentioned phases are particularly high when welding processes are applied, so after welding, the solution-annealing treatment, followed by proper cooling, is highly recommended.

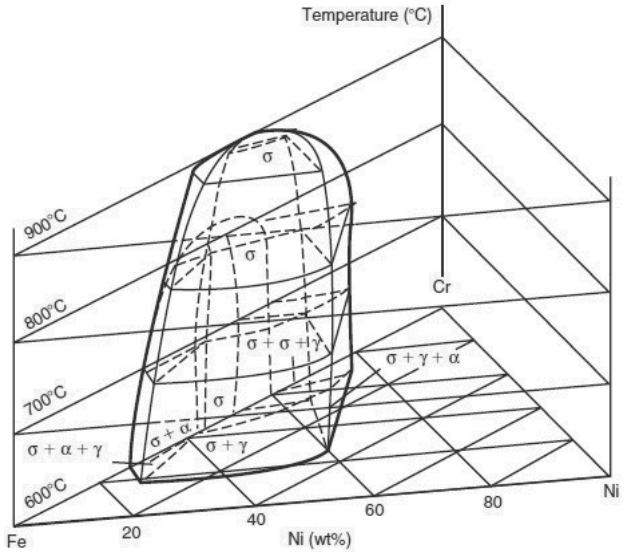

Fig. 3. Three dimensional view of the Fe-Cr-Ni equilibrium diagram [36]

Main applications of Duplex Stainless Steels include process piping systems, pumps, valves, vessels, manifolds, spools, umbilical's and flow lines, while the Superduplex grades (25 wt% Cr) are mainly seawater systems and subsea, piping, spools, tubing, flanges, umbilical's, valves, pumps, etc.

In general a good service experience is convenient to optimize the performances, however some recurring failures demonstrate that there are still quality issues to be solved. Fig. 5 [40] illustrates some statistics of failures as observed during almost 15 years.

To reduce the risk of failure, at first it is important to start with high skill and reliability at the production level, typical problems arising from the metallurgy of the alloys, too low nitrogen content and poor melting experience or during hot working (forging/rolling) due to too low surface temperature, finally performing heat treatments: heating temperature or cooling too slow, both can cause precipitation reactions.

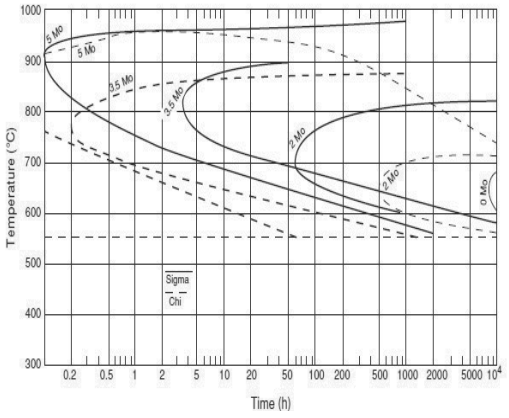

Fig. 4. Effect of molybdenum on the σ and χ-phase formation in the Fe-28% Cr-Mo system [38,39]

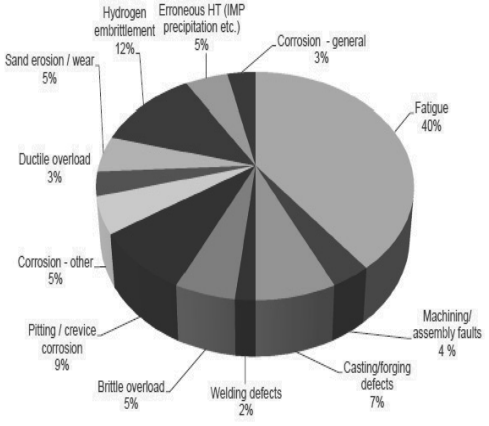

Fig. 5. Statistical results of failure analysis [40]

With the aim to contribute to better quality and performances improvements, this paper considers the microstructural properties of samples constituted by UNS S32760 SuperDuplex Stainless Steel, as a function of different supplying states, that is bars of different diameters, part of them in the annealed state and a second part strain hardened by drawing.

3. Experimental procedure

The experimental activity has been performed on samples deriving from two different sets of bars, constituted by UNS S32760 Super Duplex Stainless Steel; the bars coming from the first set are being simply annealed, whilst the bars of the second one were strain hardened by drawing. All the considered bars were part of an industrial supply to an enterprise producing parts to be used for seawater and subsea systems. The chemical composition of the annealed series of samples is indicated in Table 1, while in Table 2 the different diameters, the thermal and mechanical treatments are summarized. The strain hardened samples have correspondently the same composition of the annealed bars.

Table 1.
Chemical composition (wt. %), Fe = balance, and corrosion resistance (PRE) of the UNS S32760 Super Duplex Stainless Steel studied samples

Sample	C	Cr	Ni	Mo	Cu	N	W	Mn	Si	S	P	PRE
A	0.024	25.65	7.25	3.58	0.58	0.223	0.54	0.60	0.41	0.0009	0.022	41.032
B	0.027	25.80	6.10	3.60	0.90	0.235	0.539	0.59	0.37	0.0010	0.022	41.44
C	0.022	25.98	7.42	3.56	0.60	0.2455	0.565	0.61	0.43	0.0015	0.021	41.656
D	0.020	25.65	7.22	3.63	0.60	0.260	0.57	0.61	0.42	0.0018	0.023	41.789
E	0.019	25.38	7.47	3.65	0.91	0.230	0.58	0.61	0.51	0.0017	0.022	41.105
F	0.015	25.13	6.28	3.79	0.91	0.240	0.58	0.59	0.49	0.0019	0.023	41.49
G	0.027	25.52	6.38	3.72	0.91	0.245	0.59	0.60	0.45	0.0016	0.021	41.716
H	0.022	25.00	7.29	3.77	0.58	0.238	0.58	0.61	0.49	0.0018	0.022	41.249

Table 2.
Annealed and strain hardened samples codes and diameters

Sample type - code	Treatment state	Diameter [mm]
A: 3.138	Annealed	15.88
B: 3.137	"	28.57
C: 3.140	"	34.92
D: 33.139	"	47.62
E: 3.141	Strain Hardened	14.30
F: 3.142	"	29.57
G: 3.143	"	39.05
H: 3.144	"	45.44

Table 3.
Average PRE and mechanical properties as required for a specific application and as measured on the studied samples, S.T. strain hardened, H.T. annealed

Properties	Required	Measured S.H.	Measured H.T.
PRE	> 40	41.39	41.48
$R_{p0.2}$	> 720	815	645
UTS	> 860	895	830
El %	> 16	33	42
HRC	< 32	30.5	27.2
KV	> 35	56	63

The PRE value of the tested alloys is always higher than forty-one, meaning that all the considered samples have good corrosion resistance.

With the aim to highlight the differences between the annealed and the strain hardened samples, as well as to show the mechanism of δ ferrite decomposition with generation of σ phase precipitates, some ageing heat treatment cycles have been performed on all the type of samples. Namely the specimens have been heated in the own with an average rate of about 10°C/min at about 800°C for 30, 60 or 90 minutes, depending on the sample size.

The samples have been polished on their transverse section and prepared for microstructures observation through both Optical and Scanning Electron Microscopy (OM-SEM). The etching of the samples has been performed in different ways, traditional chemical etching using Murakami reagent (10 ml H_2O, 2 g NaOH, 2 g $K_3(CN)_6$) to highlight the mainly ferrite and austenite. However, the etching was quite difficult because of the high corrosion resistance, as indicated by PRE values of the tested samples.

Then for the correct identification of the microstructural constituents an electrochemical etching with KOH (75 g in 100 ml water, 2.5 V, about 5 s), as stated by ASTM Standard E407 has been performed. Based on this etching the austenite appears as not etched, the ferrite is coloured grey/blue like, while sigma phase will be red/brown like. Depending on local and specific situations some small changes of colours are possible.

4. Results and discussion

The samples etched with Murakami were observed by OM all at 200 magnification to have a proper comparison. The effect of this etching was more or less the same for all the samples, with the appearance of δ ferrite as dark grey, while the austenite is white. The presence of small and black precipitates was also highlighted, probably they are intermetallics phases like sigma (σ) or eventually chi (χ).

Because all the microstructures appear very similar, here in Fig. 6 is shown the sample type B. It is possible to observe a uniform distribution of ferrite and austenite, as well as the presence of small particles uniformly precipitated in the dual phased matrix.

The main difference that can be highlighted between the samples between the various samples is the grain size, in fact smaller the diameter, finer the microstructures. Noteworthy this difference can be caused by the longer cooling time for the larger diameter bars.

Even if phases having similar composition on polished surfaces when observed by SEM techniques do not offer good contrast, the observation of the etched samples with SEM was helpful to confirm and to better distinguish the phases observed by optical microscopy.

In Fig. 7, the secondary electron image shows the homogeneous distribution of ferrite and austenite, moreover the presence of very small particles is evident and, thanks to the micro-analysis, they have been identified to be σ phase. Now these micrometric sized particles appear white instead dark due to the effect of secondary electrons.

The spectrums in Figs. 8 and 9 illustrate the EDS microanalysis of the zone where σ phase is present and on the related close area with presence of austenite.

Comparing the data of Fig. 8 with those of Fig. 9, it is evident that in the first a higher concentration of Mo and Cr have been detected, while in the second one the contribution of Ni to the spectrum is more accentuated. As well-known σ phase,

constituted by Fe, Cr and Mo, can be generated during the cooling step, if the cooling rate is not fast enough, through the reaction ferrite δ → austenite γ* + sigma. Since this process is favoured by high Mo and Cr contents, the reaction preferentially will be activated in the ferritic domains. Moreover, the nucleation and the growth of σ precipitates generate Cr and Mo depletion with consequent Ni enrichment of residual ferrite grains, which becoming unstable and will be transformed in austenite (Fig. 9).

Mechanical properties and brittleness of σ phase are caused by its quite complex lattice, with high interfacial energy coupled with the absence of planes easy to slip.

Because Murakami reactive has a limited efficacy as etchant for Super Duplex grades, due to their really very high corrosion resistance, and it was difficult to highlight the grain boundary through this way.

To go over this drawback it was decided to use the electrochemical etching, more suitable for high corrosion resistant alloys. The action has been realized according to the ASTM E407 standard with KOH aqueous solution.

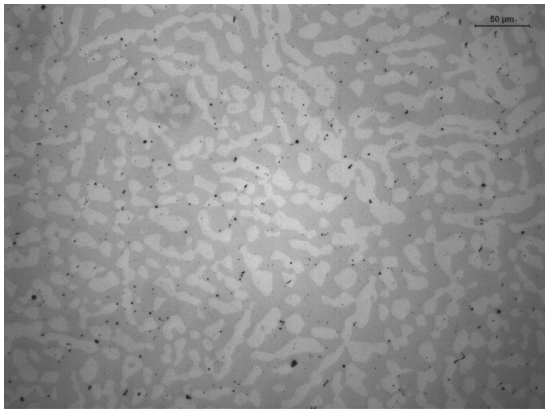

Fig. 6. Microstructure of samples type B, diameter 28.57 mm and annealed

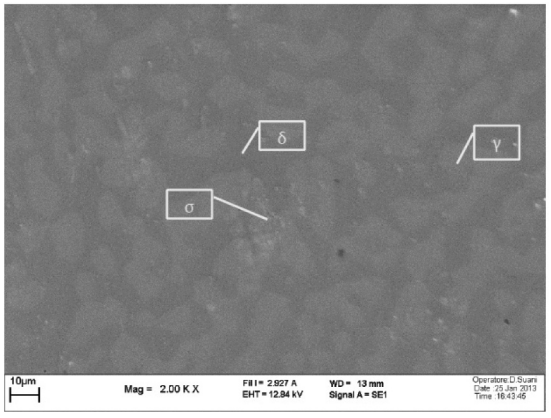

Fig. 7. Secondary electron image of sample type B, diameter 47.62 mm and annealed

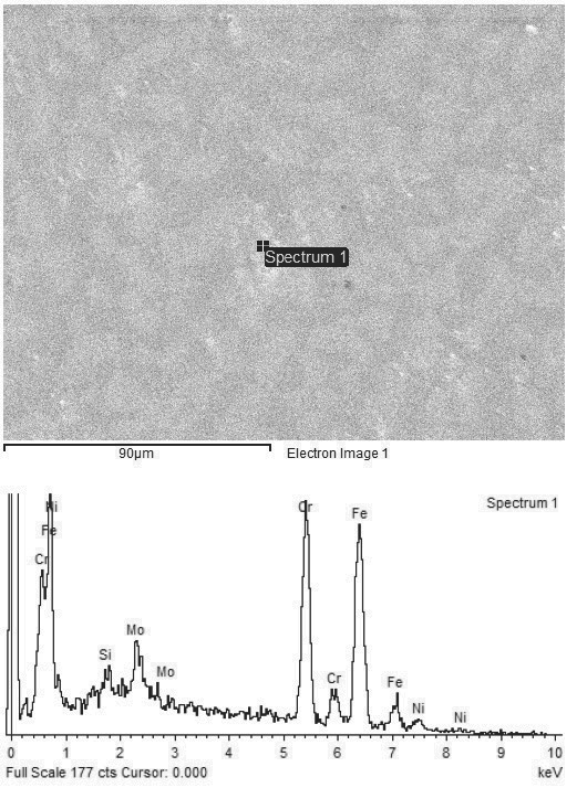

Fig. 8. EDS spectrum σ phase rich zone

In Figs. 10 to 12 microstructures of samples after electrochemical etching are shown. In these pictures the ferrite is brown, while the austenite appears mainly green/violet, however some white and bright austenite crystals are visible, evidently the composition of the austenite phase is not very homogeneous. Small changes in colors with respect to the statement of the ASTM standard can be interpreted as caused by local and specific environmental conditions.

To facilitate the comparison with Murakami etching the image of Fig. 10 is related to the same sample of Fig. 6 and at the same magnification, that is sample type B, diameter 28.57 mm and annealed. The microstructure in this case is definitely more detailed and the grain boundaries appear very well defined.

In Fig. 11 the same sample has been observed at higher magnification and important particularities became evident and a white network of austenite surrounding the ferrite grains is visible. Moreover, some areas with very small agglomerates of precipitated particles are distributed in the matrix, that is the σ phase now became evident.

The picture of Fig. 12 shows the microstructure of sample type F, that is the strain hardened bar with diameter 29.57 mm. Because the magnification is the same as in Fig. 11, a comparison of two pictures is very immediate.

In Fig. 12, the white network of austenite surrounding the ferrite grains is less visible than in Fig. 11. It seems that in the case of strain hardened samples the segregation of austenite at the grain boundary of ferrite is not so important, but some large and un-etched γ crystals are distributed in the matrix, probably are

Ni richer grains. Finally, the precipitation of σ phase also is quite reduced, that is it is very difficult to find the agglomerates of very small precipitated particles as for the annealed samples.

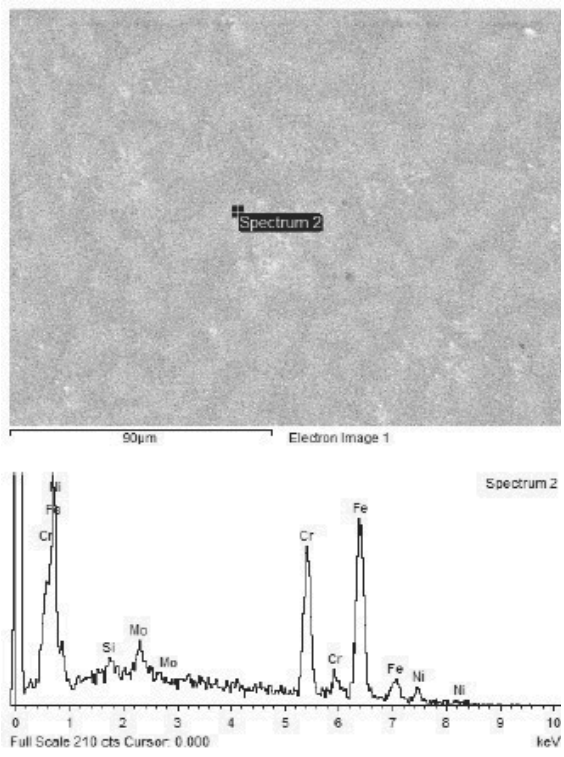

Fig. 9. EDS spectrum of region close to the precipitates of σ phase

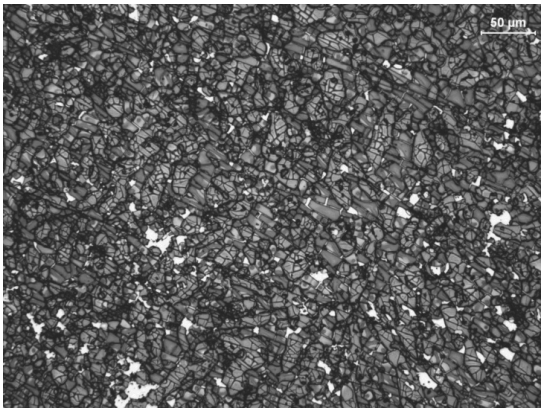

Fig. 10. Microstructure at low magnification of sample type F (strain hardened) after electrochemical etching with KOH

Further observations at SEM and EDS microanalyses were helpful for a more accurate characterization of the microstructural constituents. The picture in Fig. 13 shows the microstructure of sample type F, the same as in Fig. 12, obtained by secondary electrons, image on the left side, and as back scattering, image on the right side. Without the chromatic effects, due to the use of secondary electrons, it seems more difficult to distinguish the different phases.

However, with back scattering the different levels of grey and white allow more easier a rapid distinction of different phases.

The darker grains are δ ferrite, in fact with EDS analysis they are richer in Mo and Cr, while the light grains contain higher concentration of Ni, meaning that they are constituted by austenite and also in this case is possible to differentiate two different type of austenite, the lightest grains being the richest in Ni.

Moreover, it is possible to confirm that the precipitation of intermetallic phases in the strain hardened samples is decidedly less important than for the annealed materials and few very small particles are only visible, like the two small ones in the circled area indicated as A in Fig. 13. The EDS analysis showed that these particles are mainly constituted by Si, with a relatively high concentration of tungsten.

The different amount of σ precipitates or of other similar phases, as observed comparing the microstructures of annealed and of strain hardened series of samples, suggest that probably the annealing treatment was not performed using optimized parameters and this fact can justify also the lower and insufficient mechanical properties measured on the annealed samples, Table 3.

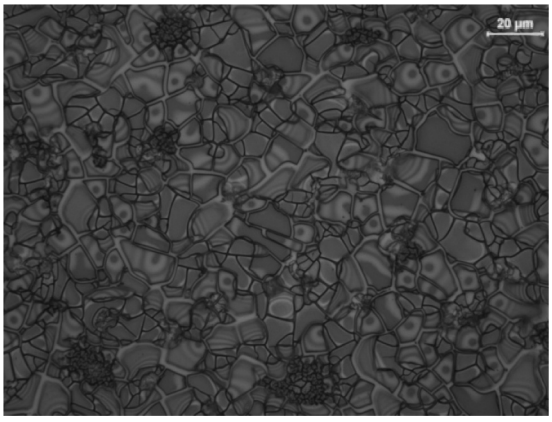

Fig. 11. Microstructure at higher magnification of sample type B, annealed, after electrochemical etching with KOH

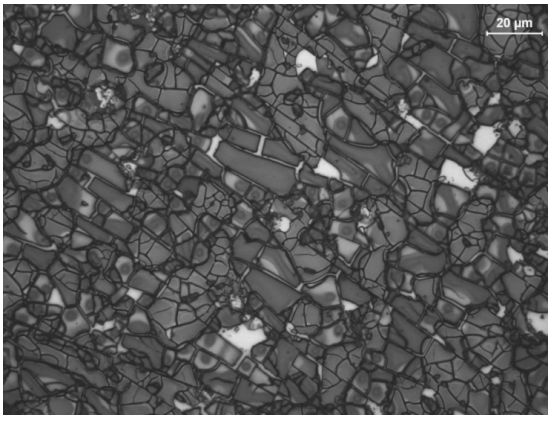

Fig. 12. Microstructure at higher magnification of sample type F, strain hardened, after electrochemical etching with KOH

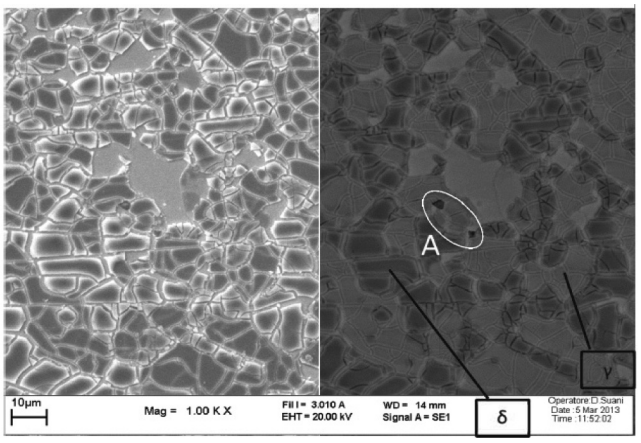

Fig. 13. Microstructure of sample type F (strain hardened) as observed at SEM by secondary electrons, left side, and as back scattering, right side.

The calculation of partition coefficients of Si, Cr, Ni and Mo wt. % as contained in ferrite and austenite phases, even with some minor changes, are in agreement with the theoretical coefficient as introduced and evaluated by J. Charles [9].

The execution of ageing treatments was helpful for obtaining indication able to support the previous sentence and to better understand the effect of heat treatments parameters on the studied alloys.

In Fig. 14 the microstructure of the sample before ageing treatment is represented as testimonial to compare the successive microstructural changes caused by treatment. Some aggregate of small grains of sigma phase are already observable in the austenite and ferrite based matrix.

After 30 minutes of ageing at 800°C the precipitation of small grains to substitute the ferrite started with consistency, grain dark brown in Fig. 15.

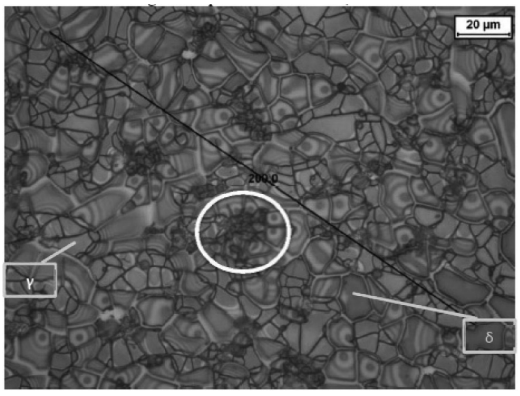

Fig. 14. Microstructure of the annealed sample before ageing treatment, some small precipitates are already present.

After 60 minutes the presence of σ phase is more evident and some γ* (white and small grains) are also visible, Fig. 16. The decomposition of ferrite in sigma and austenite seems to be completed after 1.5 h and an intimate mixture of small grains of both γ* and σ phases is quite extended, Fig. 17. The average amount of phases has been evaluated using; the primary austenite being about 54%, the mixture of γ* and σ phases being 40%, while the residual δ ferrite is 6% only.

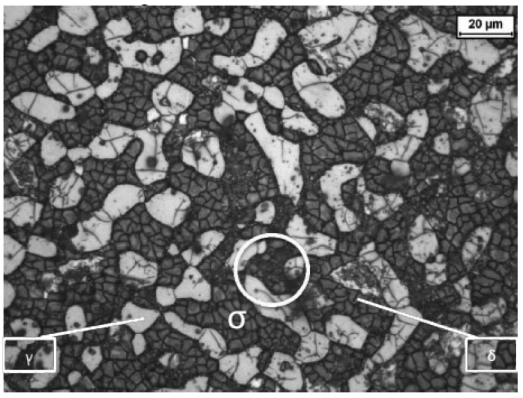

Fig. 15. The effect of 30 minutes of ageing treatment, the precipitation of σ particles initiated in different zones

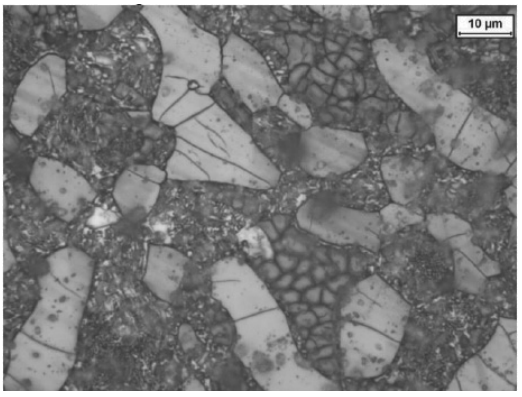

Fig. 16. The effect of 60 minutes of ageing treatment, the precipitation of σ particles now is very evident and are intimately mixed with γ* phase

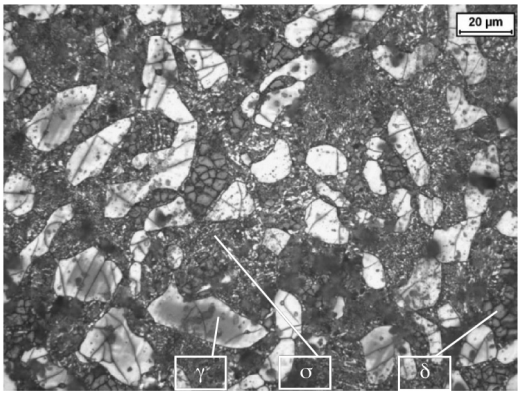

Fig. 17. The effect of 90 minutes of ageing treatment, the mixture of γ* and σ phases are replacing the ferrite, even if some residual grains of δ ferrite are still present

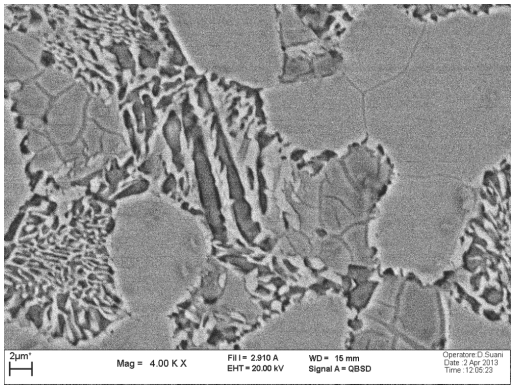

Fig. 18. SEM image of the sample after 60 minutes of ageing treatment. The intimate mixture of dark (σ) and white crystals (γ*) are substituting the original δ ferrite

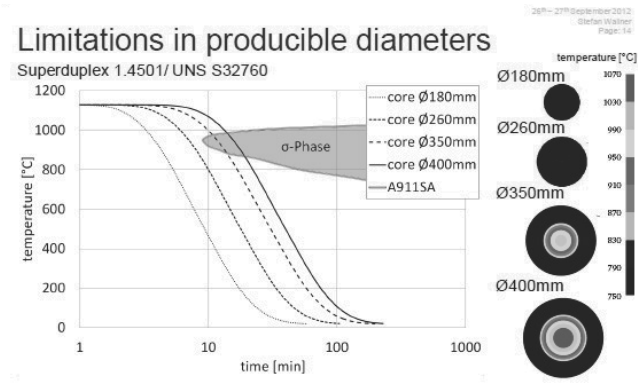

Fig. 19. Influence of bars diameter on the cooling rate and on zones of possible precipitation of σ phase [41]

Moreover, the composition of the alloys largely influence the alloy behavior during heat treatments and possible precipitations, in fact while Cr and Mo mainly are responsible for the precipitation of σ phase, nitrogen could represent a risk for the possible formation of Cr nitride, see Fig. 20 [42], which represent the shrinking of the production window.

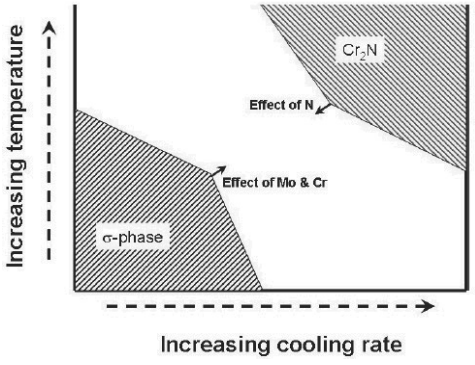

Fig. 20. Influence of Cr, Mo and N on zones of possible precipitation of sigma phase and Cr nitrides [42]

5. Conclusions

The work aimed to contribute to study the influence of strain hardening and of heat treatments on microstructural features of the grade UNS S32760 Super Duplex Stainless Steel.

Series of bars with increasing diameter have been observed and analysed after annealing treatment, as well as after strain hardening by drawing process.

Some presence of σ phase has been detected on the annealed bars, while the strain hardened one were containing only few small precipitated particles containing alloying elements, mainly Si and W, or Mn and Mo.

The precipitation of σ phase trough the decomposition of the ferrite has been caused by the execution of some ageing treatments, to demonstrate the importance of the heat treatment parameters, especially temperature and cooling rate on the microstructural constituents of Duplex Stainless Steels products and consequently on their mechanical properties and corrosion resistance.

High quality and high performance Duplex Stainless Steel products require very strict control of the composition and of all the process and treatment parameters, that is the production window is quite restricted.

References

[1] W. Reick, M. Pohl, A.F. Padilha, Steel heat treatment, metallurgy and technologies, Metalurgia International 3 (1990) 46-50.

[2] M. Rosso, M. Actis Grande, About sintering of duplex stainless steels and their properties, Proceedings of the 10th Jubilee International Science, Conference on Achievements in Mechanical and Materials Engineering, Gliwice, 2001, 499-504.

[3] M. Rosso, M. Actis Grande, D. Ornato, P. Aguiari, Mechanical characteristics and corrosion resistance properties of different PM duplex stainless steels compositions, Proceedings of PMTEC, 7/16-21, 2002, 102-109.

[4] L.A. Dobrzański, Z. Brytan, M. Actis Grande, M. Rosso, Structure and properties of sintered duplex steels, Proceedings of 12th International Conference, Achievements in Mechanical and Materials Engineering", 2003, 211-214.

[5] M Actis Grande, D. Ugues, L.A. Dobrzański, Z. Brytan, M. Rosso, Properties of vacuum sintered Duplex Stainless Steels, Proceedings of the PM2004 World Congress, Austria, 2004, 395-400.

[6] L.A. Dobrzański, Z. Brytan, M. Actis Grande, M. Rosso, E.J. Pallavicini, Properties of vacuum sintered duplex stainless steels, Proceedings of Achievements in Mechanical and Materials Engineering, 2005, 117-120.

[7] L.A. Dobrzański, Z. Brytan , M. Actis Grande, M. Rosso, Properties of duplex stainless steels made by powder metallurgy, Archives of Materials Science and Engineering 28/4 (2007) 217-233.

[8] A.F. Padilha, R.L. Plaut, P.R. Rios, stainless steel heat treatment in steel heat, Treatment handbook, Taylor and Francis Group, 2006.

[9] J. Charles, Duplex stainless steels, Les Editions de Physique, Paris, 1991, 1.
[10] J. Charles, Innovation stainless steels, AIM, Milano, 3, 29.
[11] Practical Guidelines for Fabrication of Duplex Stainless Steels, 1999, International Molybdenum Association, London, 2009, 1-98.
[12] B. Josefsson, J.O. Nilsson, A. Wilson, Duplex Stainless Steels, Les Editions de Physique, F-91944, Les Ulis Cedex, France, 1997, 67.
[13] G. Herbsleb P. Schwaab, Duplex Stainless Steels, ASM, Metals Park, Ohio, 1983, 15.
[14] L. Iturgoyen, M. Anglada, Procedure, Stainless Steels, Iron Steel Institute, Tokyo, 1991, 2, 746.
[15] J. Charles, H. Nordberg, J. Bjorkland, Applications of Stainless Steels, Jemkontorat, Sweden, 1992, 587-601.
[16] H. D. Solomen, T.M. Devine, Duplex Stainless Steels, 1983, ASM, Metals Park, OH, 693-756.
[17] A. Bäumel, Vergleichende Untersuchung nichtrostender Chrom- und Chrom-Nickel-Stähle auf interkristalline Korrosion in siedender Salpetersäure und Kupfersulfat-Schwefelsäure-Lösung. Stahl und Eisen 84 (1964) 798-807.
[18] M.A. Streicher, Microstructures and some properties of Fe-28% Cr-4% Mo alloys, Corrosion-NACE 30 (1974) 115-124.
[19] K. Lorenz, G. Medawar: Uber das Korrosionverhalten austenitischer Chrom-Nickel-(Molybdan) Stahle mit und ohne Stickstoffzusatz unter besonderer, Berucksichtigung ihrer, Beanspruchbarkeit in chloridhaltigen Losungen. Thyssenforschung 1 (1969) 97-108.
[20] J. Nowacki, P. Rybicki, Influence of heat input on corrosion resistance of SAW welded duplex joints, Journal of Achievements in Materials and Manufacturing Engineering 17 (2006) 113-116.
[21] J. Labanowski, Stress corrosion cracking susceptibility of dissimilar stainless steel welded joints, Journal of Achievements in Materials and Manufacturing Engineering 20 (2007) 255-258.
[22] J. Labanowski, Mechanical properties and corrosion resistance of dissimilar stainless steel welds, Archives of Materials Science and Engineering 28/1 (2007) 27-33.
[23] G. Niewielski, K. Radwanski, D. Kuc, The impact of deformation on structural changes of the duplex steel, Journal of Achievements in Materials and Manufacturing Engineering 23/1 (2007) 31-34.
[24] S. Topolska, J. Labanowski, Effect of microstrocture on impact toughness of duplex and superduplex stainless steels, Journal of Achievements in Materials and Manufacturing Engineering 36/2 (2009) 142-149.
[25] W. Reick, M. Pohl, A.F. Padilha, Three types of embrittlement in ferritic-austenitic duplex stainless steels, Metalurgia International 3 (1990) 46-50.
[26] M. Pohl, A.F. Padilha, O. Fossmark: Duplexstählen mit 4758-Versprödund, Materialkundlich-Technische Reihe, 9 (Gefüge und Bruch), Gebrüder Borntraeger, Berlin, 1990, 305-314.
[27] W. Reick, M. Pohl, A.F. Padilha, Recrystallization-transformation combined reactions during annealing of a cold rolled ferritic-austenitic duplex stainless steel, The Iron and Steel Institute of Japan 38 (1998) 567-571.
[28] L.A. Norström, S. Pettersson, S. Nordin, Sigma-phase embrittlement in some ferritic-austenitic stainless steels, Zeitschrift fur Werkstofftechnik 12 (1981) 229-234.
[29] A. Desestret, J. Charles, The duplex stainless steels, Stainless steels, Editions de physique, Les Ulis, France 1993, 612-658.
[30] A. Ibach, Ruhr-Universität Bochum, Fakultät für Maschinenbau, Bochum, Ph.D. Thesis, Germany, 1994.
[31] B. Weiss, R. Stickler, Phase instabilities during high temperature exposure of 316 austenitic stainless steel, Metallurgical Transactions 3 (1972) 851-866.
[32] M.B. Cortie, E.M. Jackson, Simulation of the precipitation of sigma phase in duplex stainless steels, Metallurgical and Materials Transactions A 28A (1997) 2477-2484.
[33] S. Nana, M.B. Cortie, Retardation of intermetallic phase formation in experimental superferritic stainless steels, Metallurgical and Materials Transactions A 27A (1996) 2436-2444.
[34] A.F. Padilha, F.C. Pimenta Jr., W. Reick, A comparative study on the precipitation of the sigma phase in a superferritic and in a duplex stainless steel, Zeitschrift für Metallkunde 92 (2001) 351-354.
[35] F.C. Pimenta Jr, A.F. Padilha, R.L. Plaut, Sigma phase precipitation in a superferritic stainless steel, Materials Science Forum 426-432 (2003) 1319-1324.
[36] H.J. Eckstein, Korrosionsbeständige Stähle, Deutscher Verlag für Grundstoffindustrie GmbH, Leipzig, 1990.
[37] R.M. Davison, J.D. Redmond, Practical guide to using duplex stainless steels, Materials Performance 29 (1990) 57-62.
[38] R.D. Campbell, Ferritic stainless steel welding metallurgy, Key engineering materials 69-70 (1992) 167-216.
[39] H. Brandis, H. Kieshereyer, G. Lennarrtz, Archiv für das Eisenhüttenwesen 46 (1976) 799-804.
[40] L.A. Marken, Ø. Strandmyr, Duplex Seminar and Summit, Stresa, 2012, 26-27.
[41] S. Wallner, G. Einödhofer, Duplex Seminar and Summit, Stresa, 2012, 26-27.
[42] J.O. Nilsson, Duplex Seminar and Summit, Stresa, 2012, 26-27.